THE EFFECT OF CHEMICALLY COATED NANOFIBER REINFORCEMENT ON BIOPOLYMER BASED NANOCOMPOSITES

Bei Wang, and Mohini Sain[*]

The aim of this work was to explore how various surface treatments would change the dispersion component of surface energy and acid-base character of hemp nanofibers, using inverse gas chromatography (IGC), and to investigate the effect of the incorporation of these modified nanofibers into a biopolymer matrix on the properties of their nano-composites. Bio-nanocomposite materials were prepared from poly (lactic acid) (PLA) and polyhydroxybutyrate (PHB) as the matrix, and the cellulose nanofibers extracted from hemp fiber by chemo-mechanical treatments. Cellulose fibrils have a high density of –OH groups on the surface, which have a tendency to form hydrogen bonds with adjacent fibrils, reducing interaction with the surrounding matrix. It is necessary to reduce the entanglement of the fibrils and improve their dispersion in the matrix by surface modification of fibers without deteriorating their reinforcing capability. The IGC results indicated that styrene maleic anhydride coated and ethylene-acrylic acid coated fibers improved their potential to interact with both acidic and basic resins. From transmission electron microscopy (TEM), it was shown that the nanofibers were partially dispersed in the polymer matrix. The mechanical properties of the nanocomposites were lower than those predicted by theoretical calculations for both nanofiber-reinforced biopolymers.

INTRODUCTION

Miniturization is a continuing trend in the development of technology. The prefix "nano" has become applied to new classes of materials intended for manufacturing, e.g. nano-materials and nanocomposites. Unfortunately, not many of the most recent developments of this nature are able to satisfy the core concept of sustainability. One way to address issues related to sustainability is to incorporate renewable materials as miniaturized elements of construction materials (Sain and Oksman 2006). The backbone of a plant or tree is a polymeric carbohydrate with an abundance of tiny structural entities known as "cellulose fibrils". These fibrils are comprised of different hierarchical microstructures commonly known as nano-sized microfibrils, having high structural strength and stiffness (Wang and Sain 2007). Biopolymers from renewable resources have attracted much attention lately. Renewable sources of polymeric materials offer an

answer to maintaining sustainable development of economically and ecologically attractive technology. In recent years, scientists and engineers have been working together to use the inherent strength and performance of these nano-fibrils, combined with natural green polymers, to produce a new class nano-materials.

Poly(lactic acid) (PLA) is a class of crystalline polymers with relatively high melting point (Mohanty et al. 2000). Recently PLA has been highlighted because of its availability from renewable resources such as corn and sugar beets. PLA is synthesized by the condensation polymerization of D- or L-lactic acid or ring-opening polymerization of the lactide (Lunt 1998). Advanced industrial technologies of polymerization have been developed to obtain high molecular weight pure PLA, which leads to a potential for structural materials with enough lifetime to maintain mechanical properties without rapid hydrolysis. Poly(β-hydroxybutyrate) (PHB) is a biotechnologically produced polyester that constitutes a carbon reserve in a wide variety of bacteria and has attracted much attention as a biodegradable thermoplastic polyester (Holmes 1988). However, it suffers from some disadvantages compared with conventional plastics, for example, brittleness and a narrow processability window.

Many studies have been done on extracting cellulose microfibrils from various natural sources and on using them as reinforcement in composite manufacturing (Bhatnagar and Sain 2005; Chakraborty et al. 2006; Nakagaito and Yano 2005; Sain and Bhatnagar 2003). The use of cellulose nanofibers as nanoreinforcement is a new field in nanotechnology, and as a result there are still some disadvantages. Firstly, the separation of nanoreinforcement components from natural materials and the associated processing techniques have been limited to the laboratory scale (Oksman et al. 2006). Secondly, the fiber isolation process consumes a large amount of energy, water, and chemicals. The production is time-consuming and is still associated with low yields. Thirdly, due to their strong hydrogen bonding between cellulose chains, it is necessary to reduce the entanglement of the fibrils and improve their dispersion in the solid phase polymer matrix by surface modification of nanofibers without deteriorating their reinforcing capability. It has been reported that the surface modifications of cellulose nanofibers to make them compatible with non-polar solvents or non-polar polymers. Such an approach has been attempted for polyolefins and other commodity polymers (Goussé et al. 2004). The treatment of the fibers may be by bleaching, grafting of monomers, acetylation, and so on. In this way, high performance composite materials can be processed with a good level of dispersion. Interaction of cellulose with surfactants has been another way to stabilize cellulose suspensions into non-polar systems (Heux et al. 2000).

Poor interfacial adhesion between nanofibers and the polymer matrix leads to a decline in mechanical properties of nanocomposites. In recent years a deeper under-standing has been achieved related to surface phenomena. This has led to an introduction of more sophisticated approaches, which allow for a study of thermo-dynamic and kinetic information. One technique, which has been shown to be very valuable, is inverse gas chromatography (IGC). In IGC, a solid material under investigation is used as the stationary phase. An empty column is filled with the (porous) material (adsorbent) and the adsorbate molecules in the mobile phase probe the surface of the adsorbent (Thielmann 2004). The surface energy of a material can be described by the sum of a dispersion component and a specific interaction component (Gulati and Sain 2006). The

dispersion component refers to London dispersion forces, and the specific component refers to the polar, ionic, electrical, magnetic, metallic, and acid-base interactions. Fowkes and Mostafa (1978) proposed that dispersion forces and acid-base interactions are the primary forces operating across the interface. IGC is an alternative method for measuring the changes in the thermodynamic properties of a nanofiber surface after treatment and for estimating the London dispersion component of the surface free energy of nanofibers (before and after treatment). Gulati and Sain (2006) reported that alkalization and acetylation make the hemp fibers amphoteric, thereby improving their potential to interact with both acidic and basic resins.

The goal of this work was to explore how various surface treatments would change the dispersion component of surface energy and the acid-base character of hemp nanofibers, using IGC. The cellulose nanofibers were extracted from hemp by chemo-mechanical treatments. PLA- and PHB-based nanocomposites using cellulose nanofibers were prepared by injection molding and hot compression. The cellulose nanofibers used in this study were treated by five different chemicals. Uncoated cellulose was used as a reference. Transmission and scanning electron microscopy were used to investigate the nano-structure of the nanocomposites and the dispersion of fibers within the matrix. The potential use of chemically coated nanofibers as reinforcing agents in biocomposites was also explored. The mechanical properties of the nanocomposites were studied by means of tensile testing.

EXPERIMENTAL

Materials
Matrix

Poly (lactic acid) (PLA), Nature Works^{TM} 4031D, was supplied by Cargill Dow LLC, Minneapolis, USA. The material has a density of 1.25 g/cm^3, a glass transition temperature (T_g) of 58 ^{o}C, and a melting point of 160 ^{o}C. Polyhydroxybutyrate (PHB), Biomer-P226 biodegradable polymer, was supplied by Biomer, Krailling, Germany. The material has a density of 1.17 g/cm^3 and melting point of 173 ^{o}C.

Reinforcement

The raw material used in this study was hemp fibers (*Cannabis sativa L.*) from southwestern Ontario, Canada (Hempline Inc., ON). These fibers have diameters of approximately 22-25 μm and lengths of 15-25 mm. The cellulose nanofibers were extracted from hemp fiber by chemo-mechanical treatments. Isolated nanofibers were shown to have diameters between 50-100 nm and lengths in the micrometer scale, which results in a very high aspect ratio (87.5).

Chemicals

Reagent grade chemicals were used for fiber isolation and bleaching, namely, sodium hydroxide, hydrochloric acid, sodium chlorite, chlorine dioxide, peroxide, and sulfuric acid. Michem$^®$ Prime EAA (ethylene acrylic acid) copolymer dispersions-4983R (Michelman, Inc., Cincinnati, OH) was the dispersant, which exhibits excellent adhesion

to cellulosic substrates. Styrene Maleic Anhydride resins (SMA®) from Sartomer Company (Exton, PA) are low molecular weight styrene/maleic anhydride copolymers. Hydrophobic SMA resins are used as surface sizing compounds for paper and cross-linking agents for powder coatings. Kelcoloid HVF and LVF are stabilizers used for fiber coating. Kelcoloids (International Specialty Products, Wayne, NJ) are made of propylene glycol alginates (PGA), copolymers of mannuronic and guluronic acids. The key function of PGAs is to help stabilize an emulsion or high-solids suspension. Guanidine hydrochloride, 50940 BioChemika (Fluka Chemie AG, Buchs, Switzerland) was used for the fiber coating. It was originally designed for refolding of proteins.

Methods

Nanofiber isolation

The isolation of hemp nanofibers is a multi-step process. Chemical and mechanical treatments were applied to the fiber to make nanofibers. The chemical treatment included pre-treatment, acid hydrolysis, and alkaline treatment. The mechanical treatment was comprised of two parts: cryocrushing and high pressure defibrillation. Details of the nanofiber isolation process are outlined in the author's previous publication (Wang et al. 2007).

Nanofiber chemical coating

Cellulose nanofibers were stored in water suspension after the chemo-mechanical isolation. Different types of chemicals were added to the suspension containing nanofibers in the proportion 1:2 (w/w), using an estimated weight of the cellulose nanofibers. In order to improve the dispersion of the coated nanofibers, the suspensions were prepared with continuous stirring by magnetic stirrer for 24 h at a room temperature. The suspensions containing nanofibers were freeze-dried in a Multi-Drier freeze-drying machine (Frozen in Time, Ltd.).

Processing of nanocomposites

This project was focused on synthesizing nano-biocomposites, using PLA and PHB in the solid phase, by injection molding or hot compression. A solid-phase compounding method was used to mix the freeze-dried nanofibers with PHB in a high-intensity kinetic mixer (Werner and Pfleiderer Gelimat) at 3200 rpm with tip speed of 23 m/s. Product was discharged at a pre-set temperature of 150 °C. Test samples were compression-molded with a WABASH Hot Press into sheet form. The mold temperature was 180 °C, and the pressure was 50 MPa. PLA composites containing 5 wt.% SMA-coated nanofibers were prepared by melt blending the polymer with the fiber, using a Brabender mixer (C.W. Brabender Instruments Inc., NJ). The compounding temperature was 170 °C, and the rotating screw speed was 60 rpm for 5 min. Then the compound was granulated, using a C.W. Brabender Granulator (C.W. Brabender Instruments Inc., NJ). The granulates were then pre-heated to 100 °C for 1 h and injection molded using an Engel Injection molder (Model ES-28, ON, Canada) equipped with a standard ASTM mold for tensile, flexural, and impact test specimens. The typical injection molding conditions were: injection temperature 180 °C, injection time: 8 s, cooling time 25 s, and

mold opening time 2 s. All composites contained 5 wt.% loading of nanofibers with respect to total weight of the composite.

Column preparation and IGC procedure

IGC measurements were done with a Perkin-Elmer Autosystem XL Gas Chromatograph (GC) fitted with a flame ionization detector. To ensure flash vaporization, the injection port was kept at 423 K. All stationary phases, including 2-4g uncoated hemp nanofibers (HPN) or coated-HPN, were dried in an oven at 70 °C for 24h and packed under vacuum with a vibrator into a copper column (length 33 cm and internal diameter of 4 mm) of which the end was plugged with glass wool. The columns were maintained overnight at 105 °C in a nitrogen stream to remove moisture and other volatiles from the cellulose fibers before each experiment. The columns were first cleaned with acetone before use to get rid of greases used in copper processing.

The IGC probes used in the present study were chromatography grade solvents (Sigma-Aldrich). The probes were used without further treatment. Their physicochemical properties are listed in Table 1. Helium was used as the carrier gas. The corrected flow rate of helium was 10 mL/min. Small quantities of probes were injected into the column using Hamilton syringes. Peaks were found to be symmetrical and the area under each peak was directly related the amount adsorbed/desorbed. In the present study, the temperature dependence was determined within the temperature range 40 to 100 °C. Averages of three measurements were taken to calculate retention volumes, with air as the marker.

Table 1. Physicochemical Properties of the IGC Probes used In the Present Study (Schultz et al. 1987; Guttmann 1983)

Probe	Area ($A°^2$)	γ_l^d (mJ/m^2)	DN	AN	Character
Hexane	51.5	18.4	0	0	Neutral
Heptane	57	20.3	0	0	Neutral
Octane	62.8	21.3	0	0	Neutral
Nonane	68.9	22.7	0	0	Neutral
Chloroform	44	25.9	0	23.1	Acidic
Ethyl Acetate	48	16.5	17.1	9.3	Amphoteric
Ethyl Ether	47	15	19.2	3.9	basic
Tetrahydrofuran (THF)	45	22.5	20.1	8	basic
Acetone	42.5	16.5	17	12.5	Amphoteric

Microscopy characterization

The nanostructure of the composites was examined in a transmission electron microscope (TEM), Hitachi H-7000 TEM at an acceleration voltage of 100 kV. To examine the nanocomposites, the samples were cut and polished to rectangular sheets, embedded in epoxy, and allowed to cure overnight. The final ultra-microtoming was performed with a diamond knife at room temperature, generating foils approximately 90 nm in thickness. These foils were gathered onto Cu grids.

A scanning electron microscope (JEOL JSM-840, Tokyo, Japan) (SEM) was used as a routine for microstructural analysis of the nanofibers with and without surface

coatings. All images were taken at an accelerating voltage of 15 kV. The sample surfaces were coated with a thin layer of gold on the surface, using an Edwards S150B sputter coater (BOC Edwards, Wilmington, MA) to provide electrical conductivity.

Tensile testing

The mechanical behavior of nanofiber-blend-PHB film or nanofiber-blend-PLA nanocomposite was tested by an Instron 5860 (Grove City, PA) in tensile mode with a load cell of 2 kN or 30 kN in accordance with ASTM D 638. The specimens were cut in a dumbbell shape with a die ASTM D 638 (type V). Tensile tests were performed at a crosshead speed of 2.5 mm/min. The values reported in this work result from the average of at least 5 measurements.

BACKGROUND

Determination of the Acid-Base Characteristics of Lignocellulosic Surfaces by IGC

The surface energy of a material can be described by the sum of the London dispersion component and specific interactions. Thus, the work of adhesion can be written as,

$$W_a = W_a^d + W_a^{AB} \tag{1}$$

where W_a, W_a^d, and W_a^{AB} are the total work of adhesion, the work of adhesion due to dispersion forces and acid-base interactions, respectively. Acid-base interactions are useful for surface modification (Dwight et al. 1990). Hence, in order to design new modification methods for improving fiber-matrix adhesion and meaningful interpretation of the existing methods, quantitative determination of surface acid-base characteristics of natural fibers is important. Data generated in this study explored surface modification for lignocellulosic fibers and their compatibilization with biopolymers.

Background of IGC

IGC has become a widely used technique to characterize the surface properties of organic and inorganic materials. Acid-base probes are used to measure the acid-base characteristics of the solid surface, and saturated n-alkane probes are used to measure the dispersion component of the surface energy of interaction. In the present study, retention times of saturated n-alkane and acid-base probes injected at infinite dilution were used to calculate the dispersion component (γ_s^d) of the surface energy, the free energy of adsorption (ΔG^{AB}), and the enthalpy of adsorption (ΔH^{AB}) corresponding to acid-base surface interactions. Papier's approach, as described by Schultz et al. (1987; 1991), was used to estimate the acceptor (K_A) and donor (K_D) parameters of the test substrates.

The fundamental parameter in the IGC measurements is the specific retention volume, V_n, defined as the volume of carrier gas required to elute a probe from a column. V_n is related to experimental variables by the following equation,

$$V_n = F^*(T_r - T_o) \tag{2}$$

where T_r and T_o are the retention times of the probe and the air marker, respectively; F^* is the corrected flow rate of the carrier gas, defined as,

$$F^* = FJ \tag{3}$$

where F is the corrected gas flow rate in mL/min; J is the correction factor for the gas compressibility,

$$J = 1.5 \ [(P_i/P_o)^2 - 1]/[(P_i - P_o)^3 - 1] \tag{4}$$

where P_o is the carrier gas pressure at the column outlet, and P_i is the carrier gas pressure at the column inlet.

The interaction of neutral probes, such as saturated n-alkanes, with the substrate material is dominated by the van der Waals dispersion forces of interaction. Molar free energy of adsorption is related to net retention volume by the following relation,

$$\Delta G = RT \ln(V_n) + C \tag{5}$$

where R is the gas constant, T is the column absolute temperature, and the value of C depends on the reference state. The free energy of adsorption is related to work of adhesion by the following relation (Mukhopadhyay and Schreiber 1995),

$$\Delta G = NaW_a = 2Na(\gamma_s^d)^{1/2}(\gamma_l^d)^{1/2} + C \tag{6}$$

where N is Avogadro's number; a is the surface area of a single probe; W_a is the work of adhesion; γ_l^d is the dispersion component of the surface energy of the probe; and γ_s^d is the dispersion component of the total surface energy of the interacting solid. Combining equation (5) and (6), we get:

$$RT \ln(V_n) = 2Na(\gamma_s^d)^{1/2}(\gamma_l^d)^{1/2} \tag{7}$$

A plot of $RT \ln(V_n)$ versus $2Na(\gamma_l^d)^{1/2}$ should give a straight line with slope $(\gamma_s^d)^{1/2}$ in the case of probes interacting only due to dispersion component of surface energy. From the slope of the straight line γ_s^d can be calculated.

The free energy of adsorption (ΔG^{AB}) corresponding to the specific acid-base interactions is related to the enthalpy of adsorption (ΔH^{AB}) by,

$$\Delta G^{AB} = \Delta H^{AB} - T\Delta S^{AB} \tag{8}$$

where ΔS^{AB} is the entropy of adsorption corresponding to the specific acid-base interactions. A plot of ΔG^{AB} versus T (temperature) should yield a straight line with intercept equal to ΔH^{AB}. The enthalpy of adsorption corresponding to the specific acid-

base interaction is related to the acceptor and donor parameters, K_A and K_D of the fibers. According to Saint-Flour and Papirer (1982),

$$\Delta H^{AB} = K_A DN + K_D AN \tag{9}$$

where DN and AN are the donor and acceptor numbers, respectively, of the acid-base probe as defined by Guttmann (1983). A plot of ΔH^{AB}/AN versus DN/AN should yield a straight line with slope K_A and intercept K_D. According to Schultz (1987) the specific interaction parameter, I, for acid-base interactions can be defined as,

$$I = K_A{}^f K_D{}^m + K_A{}^m K_D{}^f \tag{10}$$

where the superscripts f and m refer to fiber and matrix, respectively.

RESULTS AND DISCUSSION

Dispersion Component of The Surface Energy

Preliminary experiments were performed on the coated and uncoated cellulose powders to determine the optimum chromatographic conditions for reproducible measurements of the retention times of the probes. The chromatographic peak shape of each probe had to be as symmetrical as possible. The dispersion component of uncoated and chemically coated hemp fibers was calculated from a plot of RT $\ln(V_n)$ versus $2Na(\gamma_l{}^d)^{1/2}$. The values for the dispersion component, $\gamma_s{}^d$, of the surface energy at different temperatures are summarized in Table 2.

Table 2. Dispersion Component, $\gamma_s{}^d$, of the Surface Energy of Lignocellulosic Particles at Different Temperatures

Material	$\gamma_s{}^d$ (mJ/m^2)			
	313K	333K	353K	373K
Cellulose (Dorris and Gray 1979)	48	44	40	36
Uncoated HPN	42	40	34	28
SMA-Coated HPN	44	41	39	36
HVF-Coated HPN	46	44	43	38
LVF-Coated HPN	44	42	40	33
EAA-Coated HPN	46	43	41	37
Guanidium Hydrochloride Coated HPN	50	47	44	41
PLA	32	29	28	27
PHB	51	47	43	40
HPN: hemp nanofibers				

The dispersion component of resin was also calculated similarly. The linear relationship vs. n-alkane chain length illustrates that this technique works well in case of natural fibers. Chemical treatments had the effect of increasing their respective $\gamma_s{}^d$ values toward that of the cellulose powder. This is likely due to the dissolution of low energy surface impurities and surface exposure of relatively higher energy cellulose. In the

present study, the temperature dependence was determined in the temperature range 40 to 100 °C. Chemically coated fibers showed a negative temperature coefficient over this entire range due to chemical rearrangements. The London dispersion component was affected by the type of polymers and the treatment of fibers.

Acid-base Interactions of the Surface Energy

Values of the free energy of adsorption, ΔG^{AB}, corresponding to surface acid-base interactions are summarized in Table 3. The corresponding values of the enthalpy of adsorption, ΔH^{AB}, determined from the plots of ΔG^{AB} as a function of temperature (T) for all the probes in all cases, are given in Table 4. Some probes showed a negative acid-base free energy and enthalpy of adsorption on the cellulose. For example, the acid-base interaction between HVF-coated HPN (hemp nanofibers) and the ethyl ether probe was not favorable for adsorption. Considering that ethyl ether is basic (DN = 19.2), and the HVF-coated HPN used in this study was found to have a basic characteristic ($K_D = 0.22$), this result is not surprising. A comparison of the enthalpy of adsorption between uncoated and coated fibers indicated that the interactions between the probes and SMA- and EAA-coated HPN were greater than those observed between the probes and uncoated HPN. The uncoated HPN had relatively low donor ($K_D = 0.31$) and acceptor ($K_A = 0.19$) parameters compared to the donor ($K_D = 0.77$) and acceptor ($K_A = 0.34$) parameters of SMA-coated HPN. The significant increase in the acceptor parameter K_A suggests that coated fiber may interact more strongly with a matrix (Marcovich et al. 1996).

The K_A and K_D values for the respective fibers were estimated from the slope and intercept of the respective linear regression lines of $\Delta H^{AB}/AN$ as a function of DN/AN. These values are summarized in Table 5. Qualitatively, SMA-coated HPN showed relatively higher acid-base characteristics than uncoated HPN. A similar trend was observed in the case of EAA-coated HPN compared with uncoated HPN. The uncoated, SMA-coated, HVF-coated, and LVF-coated HPN showed a basic surface characteristic. K_A and K_D values appear to be consistent with the molecular structure of cellulose, where the hydrogen atoms in the hydroxyl groups act as electron acceptors and the oxygen atoms in the glycosidic linkages and hydroxyl groups act as electron donors. The EAA-coated HPN showed an amphoteric surface characteristic, and guanidium hydrochloride coated HPN showed a predominantly acidic characteristic. The relatively high K_A value indicates a surface that is rich in hydroxyl groups.

The surfaces of uncoated and chemically coated fibers were enriched by different classes of chemicals and extractives. Hemp fibers were found to be basic, which is probably due to presence of triglycerides, which exhibit a pronounced basic character (Tshabalala 1997). The removal of extractives and hemicellulose by chemical treatments had the effect of increasing the dispersion component of the surface energy of the HPN. The polymer matrix PLA used in this study was found to have an acidic character. By contrast, PHB showed a predominantly basic character, according to the K_A and K_D values.

Values of the specific interaction parameter, as defined by Schultz et al. (1987), were calculated for each type of fiber and resin combination. These values are shown in Table 6. Acid-base interactions with PLA increased by SMA- and EAA-coated HPN, and a very similar trend was observed for PHB matrix. EAA copolymers were used as a

dispersant in this study, bringing together in one product the benefits of both ethylene and acrylic acid. The crystalline structure of ethylene provides the barrier properties, flexibility, and resistance to water and chemicals. The acrylic acid comonomer imparts improved adhesion, hot-tack strength, and optical clarity. The nanofiber suspension containing EAA dispersant remains homogeneous indefinitely. It has excellent adhesion to cellulose and other polar substrates due to the high content of acrylic acid in the base copolymer. The EAA dispersant also exhibits outstanding adhesion to polyethylene and other plastics. Styrene maleic anhydride (SMA) resins are low molecular weight styrene/maleic anhydride copolymers. Altering the styrene to maleic anhydride ratio changes the hydrophilic/hydrophobic balance of the polymer. At their most hydrophilic, SMA resins form high solids solutions and can be used to produce fiber dispersions. These results are of special practical importance because surface acid-base interactions may be implicated in the adhesion of coatings and finishes to polymer and other lignocellulosic fibers. Adsorption occurred only when there was an exothermic interracial acid-base interaction. The present paper is only focused on the material structure and mechanical properties of SMA-coated HPN nanocomposites. The properties of EAA-coated HPN nanocomposites were discussed in the author's previous publication (Wang and Sain 2007).

Material Structure

Figure 1 presents typical pictures of freeze-dried HPN. Figure 1(a) is a SEM image of uncoated HPN. Each particle of HPN is an aggregation of cellulose fibers due to the strong hydrogen bonds of adjacent molecules. The size of the fiber bundle is at the μm level. Figure 1(b) shows a picture of SMA-coated HPN with a well-organized web-like structure. The morphology of coated HPN appears distinguishable compared to uncoated HPN. The SMA-coated fibers formed loose networks during freeze drying. It is proved that SMA could reduce the entanglement of the nanofibers.
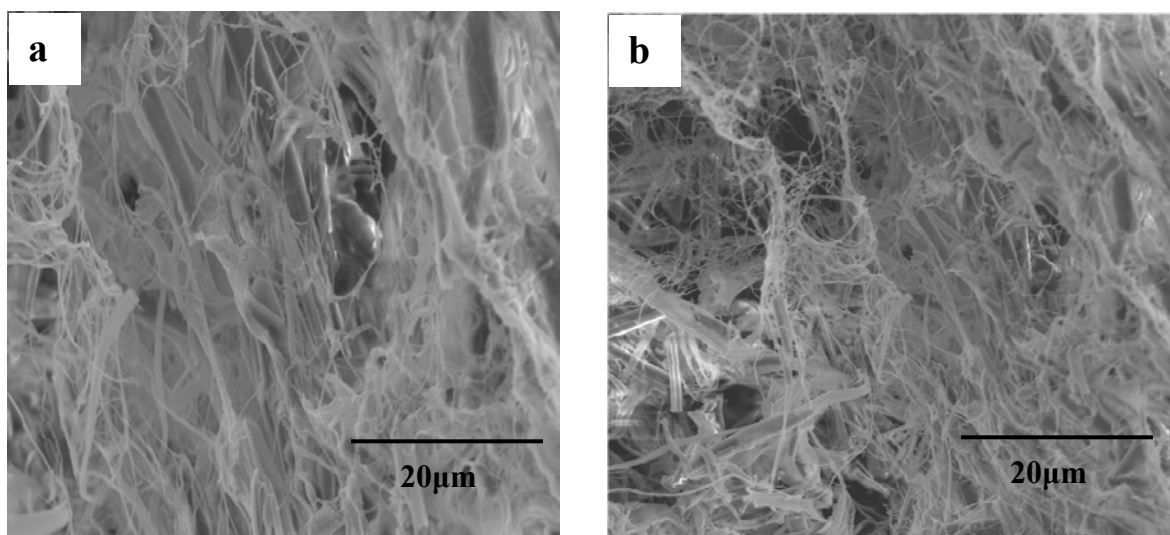
Fig. 1. Scanning electron micrographs of freeze-dried HPN samples: (a) uncoated and (b) SMA coated.

Table 3. Free Energy of Adsorption, ΔG^{AB}, of the Acid-Base Probes at Different Temperatures

Substrate/Probe	ΔG^{AB} (KJ.mol^{-1})			
	313K	333K	353K	373K
Uncoated HPN				
Chloroform	3.76	1.50	-0.86	-2.37
Ethyl Acetate	5.36	4.61	3.25	1.66
Ethyl Ether	3.15	-0.20	-0.52	-3.06
Tetrahydrofuran (THF)	4.40	2.88	1.52	-1.32
Acetone	4.61	2.23	0.07	-2.37
SMA-Coated HPN				
Chloroform	12.86	12.68	8.89	5.55
Ethyl Acetate	12.10	10.79	8.76	6.58
Ethyl Ether	8.20	7.45	6.39	5.42
Tetrahydrofuran (THF)	13.07	12.55	12.21	11.43
Acetone	12.86	11.91	11.28	9.21
HVF-Coated HPN				
Chloroform	2.30	1.10	-1.63	-4.38
Ethyl Acetate	2.07	0.90	-0.80	-1.64
Ethyl Ether	-1.05	-3.43	-7.34	-9.93
Tetrahydrofuran (THF)	2.31	0.41	-0.05	-0.97
Acetone	1.64	-0.14	-1.63	-4.63
LVF-Coated HPN				
Chloroform	3.59	2.64	-0.17	-1.49
Ethyl Acetate	1.79	0.86	0.36	-0.73
Ethyl Ether	-0.07	-1.20	-3.40	-4.53
Tetrahydrofuran (THF)	1.86	0.95	0.33	-0.26
Acetone	2.73	1.76	1.35	0.27
EAA-Coated HPN				
Chloroform	12.70	11.33	10.66	9.83
Ethyl Acetate	11.71	10.99	9.99	9.08
Ethyl Ether	10.29	8.13	7.00	6.37
Tetrahydrofuran (THF)	13.56	12.47	11.54	10.78
Acetone	9.96	9.35	8.79	8.71
Guanidium Hydrochloride Coated HPN				
Chloroform	-1.87	-3.41	-4.81	-5.09
Ethyl Acetate	-3.05	-3.57	-3.89	-4.04
Ethyl Ether	-4.26	-4.54	-4.81	-5.09
Tetrahydrofuran (THF)	-3.47	-3.48	-3.49	-3.50
Acetone	2.96	2.87	2.71	2.62

*ncsu.edu/**bioresources***

Table 4. Enthalpy of Adsorption, ΔH^{AB}

Probe	ΔH^{AB} (KJ.mol^{-1})					
	Uncoated HPN	SMA-Coated HPN	HVF-Coated HPN	LVF-Coated HPN	EAA-Coated HPN	Guanidium Hydrochloride Coated HPN
Chloroform	5.70	16.43	5.04	5.65	13.45	1.04
Ethyl Acetate	6.83	14.20	3.34	2.58	12.67	2.81
Ethyl Ether	4.58	9.21	2.20	1.59	11.17	3.98
Tetrahydrofuran (THF)	6.50	13.63	3.00	2.47	14.41	3.46
Acetone	6.91	14.21	3.88	3.47	10.28	3.09

Table 5. Surface Acid-Base Characteristics, K_A and K_D

Material	K_A (a.u.)	K_D (a.u.)
Uncoated HPN	0.19	0.31
SMA-Coated HPN	0.34	0.77
HVF-Coated HPN	0.07	0.22
LVF-Coated HPN	0.04	0.23
EAA-Coated HPN	0.49	0.45
Guanidium Hydrochloride Coated HPN	0.20	0.02
PLA	0.18	0.12
PHB	0.22	0.69

Table 6. Values of Specific Interaction Parameter

$I = K_A^f K_D^m + K_A^m K_D^f$	PLA	PHB
Uncoated HPN	0.08	0.20
SMA-Coated HPN	0.18	0.41
HVF-Coated HPN	0.05	0.10
LVF-Coated HPN	0.05	0.08
EAA-Coated HPN	0.14	0.44
Guanidium Hydrochloride Coated HPN	0.03	0.14

The processing of cellulose nanocomposites renders several challenges. The major difficulty is to achieve uniformly dispersed nanofibers in the polymer matrix. The nanofibers have a very large surface-to-volume ratio and have a tendency to aggregate when dried. The injected composites were examined using a transmission electron microscope (TEM) to study the composite morphology at nanoscale. Figure 2(a) shows an overview picture of the PLA/SMA-coated HPN composite. It was difficult to see any cellulose nanofibers in this sample. There are some dark spots, indicating that the nanofibers were not uniformly dispersed in the PLA matrix, and it is possible that the cellulose was degraded during processing. In Fig. 2(b) a more detailed view of the composite with PLA is shown. It can be seen that the nanofibers were partly dispersed in PLA. Agglomerates were present in the PLA/SMA-coated HPN nanocomposite. The structure can therefore not be described as fully networked. The dispersion and distribution of nanofibers can be affected and improved by optimizing the chemical surface treatments and the compounding process. Figure 2(b) shows the presence of a

non-homogeneous structure of nanofibers in the PLA based nanocomposites. This fact will be reflected in the mechanical properties, since there is a strong link between the morphology of nanocomposites and the improvement in properties of the polymer matrix.
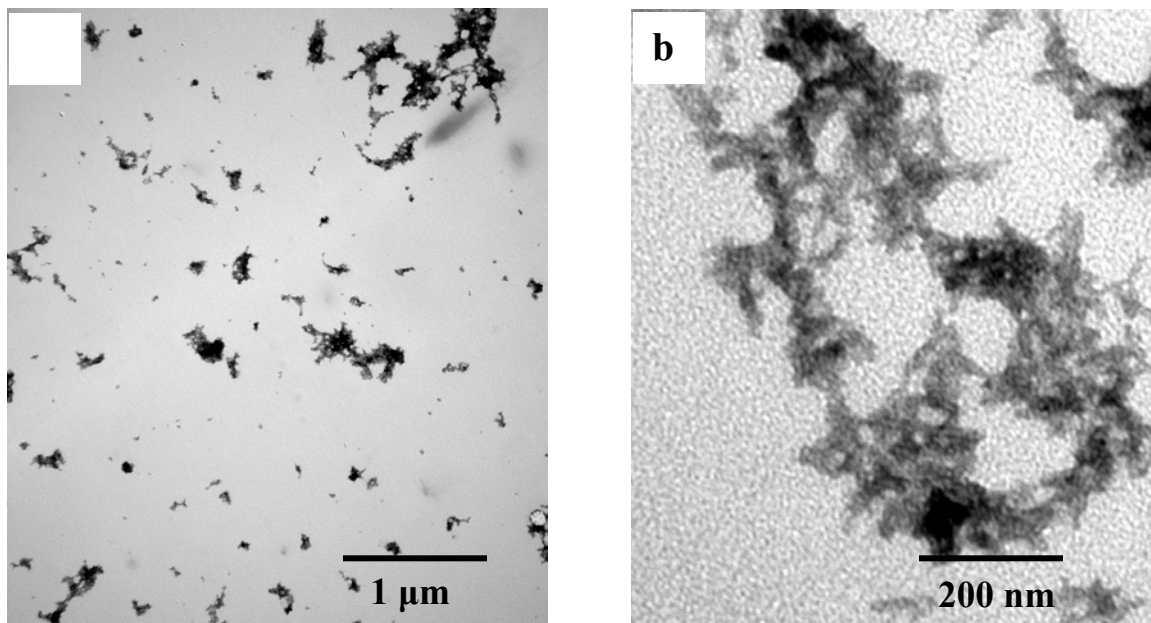
Fig. 2. Transmission electron micrograph of the PLA/SMA-coated HPN composites: (a) an overview and (b) detailed view.

Mechanical Properties of Nanocomposites

The chemical surface modifications of cellulose fibers were studied with the aim of improving their interfacial compatibility with PLA and PHB, that is, to enhance the mechanical properties of the ensuing composite. The mechanical properties of the prepared nanocomposites are presented in Table 7. There were some improvements in the properties of the nanocomposite materials, compared to pure PLA and PHB. Table 7 also shows that the improvements were similar for both nanoreinforcements. The PHB/SMA-coated HPN nanocomposite showed a 17% increase in the yield strength and a 24.5% increase in modulus in comparison to PHB/uncoated HPN nanocomposite. There was a 35% increase in the yield strength and a 37% increase in modulus relative to pure PHB. The PLA/SMA-coated HPN nanocomposite showed only a 3% increase in tensile strength and a 7% increase in modulus compared to PLA/uncoated HPN. There was a 8.6% increase in tensile strength and a 10% increase in modulus, compared to pure PLA. These results were lower than expected. Theoretical calculations were therefore performed in order to better understand the results and to see the potential effect of both nanoreinforcements.

Table 7. Tensile Properties of the Nanocomposites.

Materials	Max. Stress (MPa)	S.D.	E-Modulus (GPa)	S.D.
PHB	15.32	1.00	1.41	0.16
PHB/Uncoated HPN	17.68	1.68	1.55	0.11
PHB/SMA-coated HPN	20.68	6.66	1.93	1.25
PLA	65.49	0.21	2.72	0.09
PLA/Uncoated HPN	68.97	0.40	2.80	0.06
PLA/SMA-coated HPN	71.14	0.64	2.99	0.01

The Halpin-Tsai equation was used to calculate the theoretical tensile modulus for the two nanocomposite materials, see Eq. (11) – Eq. (14) (Agarwal and Broutman 1990),

$$E = E_m (1 + \zeta \eta \Phi)/(1-\eta \Phi) \tag{11}$$

where E_m is the Young's modulus of the matrix, E_f represents Young's modulus of the filler, ζ is a shape parameter dependent upon filler geometry, orientation, and loading direction, and η is given by,

$$\eta = (E_f/E_m-1) / (E_f/E_m+1) \tag{12}$$

$$\zeta = 2 \times \text{Length/Diameter} \tag{13}$$

$$\Phi = \text{volume fraction} \tag{14}$$

The Halpin-Tsai equation is normally used to predict the modulus for aligned fiber composites, but it has been used before to predict the modulus of nanocomposites (Wu et al. 2004; Fornes and Paul 2003). It was chosen because it demanded the least amount of assumptions to be made about the materials. The Halpin-Tsai equation can only be applied to predict the modulus of fiber/matrix nanocomposites in the range of low fiber volume fractions. At high filler concentration, the predicted value is lower than the experimental data. It is assumed that the filler apparent volume is related to the dispersion of filler, and that the larger apparent volume may originate in better dispersion, which results in a higher modulus of the composite. When the predicted values at filler volume concentrations of less than 6%, it is well fitted to the experimental data (Wu et al. 2004). By comparing model predictions with the two-dimensional finite element calculations for discontinuous oriented square fiber-reinforced composites, Ashton et al. (1969) deter-mined that $\zeta = 2$ (length/diameter of the fiber) = 2 × aspect ratio provided good agreement for longitudinal modulus.

The volume fraction of each nanoreinforcement was calculated using Eq. (15) (Luo and Daniel 2003),

$$\Phi_f = (w_f/\rho_f)/(\ (w_f/\rho_f) + (1 - w_f)/\rho_m) \tag{15}$$

where, $w_f = 5\%$, $\rho_{cellulose} = 1.58$ g/cm^3 (Ganster et al. 1999), $\rho_{SMA\text{-}coated\ HPN} = 1.70$ g/cm^3, $\rho_{PLA} = 1.25$ g/cm^3, and $\rho_{PHB} = 1.17$ g/cm^3. The volume fractions for the PLA/uncoated HPN and the PLA/SMA-coated HPN were determined to be 4% and 3.7%, respectively. The volume fraction for the PHB/uncoated HPN and the PHB/SMA-coated HPN were 3.75% and 3.5%, respectively. The following data were used in the calculation: $E_{PLA} = 1.7$ GPa, $E_{PHB} = 1.0$ GPa, $E_{cellulose} = 167.5$ GPa (Petersson and Oksman 2006), aspect ratio of uncoated HPN is 88, and aspect ratio of SMA-coated HPN is 82 (Wang et al. 2007). A comparison between the theoretical and experimental results can be seen in Fig. 3. When comparing the results, one has to keep in mind that theoretical calculations are based on PLA/cellulose and PHB/cellulose systems, where the nanoreinforcement is aligned in the longitudinal direction and has perfect interfacial adhesion to the matrix. From Fig. 3, we can draw the conclusion that both systems have large potentials for strength development, which this experiment was unable to reach. One can also see that the PLA system has the largest potential and that the PLA/nanofiber system, due to its agglomerated structure, was farthest away from its theoretical value. When it comes to the PLA/uncoated HPN and the PLA/SMA-coated HPN system, the uncoated nanofiber PLA system should have higher theoretical tensile strength value, compared to the SMA coated nanofiber PLA system, due to its lower volume fraction. In contrast, the chemical treatments on the fiber surface increased the interfacial adhesion between fiber and matrix; the experimental results showed the PLA/SMA-coated HPN system as having higher tensile properties.
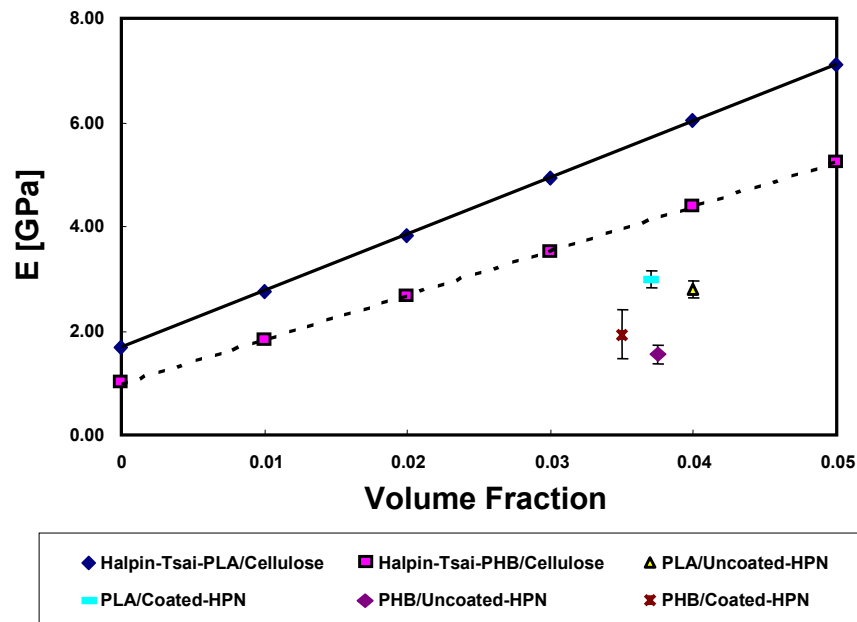
Fig. 3. Experimentally measured tensile modulus data compared to theoretical predictions by Halpin-Tsai.

CONCLUSIONS

1. Inverse gas chromatography (IGC) at infinite dilution has proven to be a convenient tool for measurement of surface energy and acid-base characteristics of natural fibers and polymer matrix. Changes in final properties of the composites due to the effect of various chemical treatments on the fiber surface can also be explained using this technique. Acid-base interactions with PLA were increased by SMA- and EAA-coated HPN, and the same trend was observed for the PHB matrix.
2. SEM pictures showed SMA-coated HPN having a well-organized web-like structure and proved that the size of nanofibers is indeed in the nano-level. Current TEM pictures showed the presence of a non-homogeneous structure of nanofibers in the PLA based nanocomposites. The properties shown here will most probably be improved if it is possible to disperse the nanofibers more evenly within the polymer matrix. A uniform nanofiber dispersion in a matrix, coupled with a high aspect ratio of the nanofibers will indicate a strong potential for the use of these biocom-posite films.
3. In both PLA and PHB systems, the SMA-coated HPN as the reinforcement enhanced the mechanical properties over the systems containing uncoated HPN or pure polymer. The theoretical calculations made in this article showed that the PLA has the largest potential to improve the mechanical properties, compared to the PHB system. This experiment was a step in the direction of creating fully renewable biopolymer based nanocomposites.

ACKNOWLEDGMENTS

REFERENCES CITED

Agarwal, B. D., and Broutman, L. J. (1990). *Analysis and Performance of Fiber Composites*, 2nd Edition, John Wiley & Sons, Inc., New York.

Ashton, J. E., Halpin, J. C., and Petit, P. H. (1969). *Primer on Composite Materials: Analysis*, Techomic Pub. Co., Stamford.

Bhatnagar, A., and Sain, M. (2005). "Processing of cellulose nanofiber-reinforced composites," *J. Reinf. Plast. Comp.* 24, 1259-1268.

Chakraborty, A., Sain, M., and Kortschot, M. (2006). "Reinforcing potential of wood pulp-derived microfibres in a PVA matrix," *HOLZFORSCHUNG* 60(1), 53-58.

Dorris, G. M., and Gray, D.G. (1979). "Adsorption spreading pressure and London force interactions of hydrocarbons on cellulose and wood fiber surfaces," *J. Colloid Interface Sci.* 71: 93-110.

Dwight, D. W., Fowkes, F. M., Cole, D. A., Kulp, M. J., Sabat, P. J., Salvati, L., and Huang, T.C. (1990). "Acid-base interfaces in fiber-reinforced polymer composites," *J. Adhes. Sci. Technol.* 4(8), 619-632.

Fornes, T. D., and Paul, D. R. (2003) "Modeling properties of nylon 6/clay nanocomposites using composite theories," *Polymer* 44, 4493-5013.

Fowkes, F. M., and Mostafa, M. A. (1978). "Acid-base interactions in polymer. adsorption," *Ind. Eng. Chem. Prod. Res. Dev.* 17: 3-7.

Ganster, J., and Fink, H-P (1999). *Physical Constants of Cellulose*, 4th ed., Vol. 1, J. Brandrup, E. H. Immergut, and E. A. Grulke (eds.), Polymer Handbook, John Wiley & Sons, Inc., New York.

Goussé, C., Chanzy, H., Cerrada, M. L., and Fleury, E. (2004). "Surface silylation of cellulose microfibrils: preparation and rheological properties," *Polymer* 45: 1569-1575.

Gulati, D., and Sain, M. (2006). "Surface characteristics of untreated and modified natural fibers," *Polym. Eng. Sci.* 46(3): 269-273.

Guttmann, V. (1983). *The Donor Acceptor Approach to Molecular Interactions*, Plenum Press, New York.

Heux, L., Chauve, G., and Bonini, C. (2000). "Nonflocculating and chiral-nematic self-ordering of cellulose microcrystals suspensions in nonpolar solvents," *Langmuir* 16(21), 8210-8212.

Holmes, P. A. (1988). *Development of Crystalline Polymers*, Vol. 2, D.C. Bassett, ed., Elservier, London.

Lavielle, L., and Schultz, J. (1991). "Surface properties of carbon fibers determined by inverse gas chromatography: role of pretreatment," *Langmuir* 7(5), 978-981.

Lunt, J. (1998) "Large-scale production, properties and commercial application of polylactic acid polymers," *Polym. Degrad. Stabil.* 59, 145-151.

Luo, J-J, and Daniel, I. M., (2003) "Characterization and modeling of mechanical behavior of polymer/clay nanocomposites," *Compos. Sci. Technol.* 63, 1607-1616.

Marcovich, N. E., Reboredo, M. M., and Aranguren, M. I. (1996). "Composites from sawdust and unsaturated polyester," *J. Appl. Polym. Sci.* 61(1), 119-124.

Mohanty, A. K., Misra, M., and Hinrichsen, G. (2000). "Biofibres, biodegradable polymers and biocomposites: an overview," *Macromol. Mater. Eng.* 276/277, 1-24.

Mukhopadhyay, P., and Schreiber, H. P. (1995) "Aspects of acid-base interactions and use of inverse gas chromatography," *Colloid. Surface. A* 100(1-3), 47-71.

Nakagaito, A. N., and Yano, H. (2005). "Novel high-strength biocomposites based on microfibrillated cellulose having nano-order-unit web-like network structure," *Appl. Phys. A.* 80, 155-159.

Oksman, K., Mathew, A. P., Bondeson, D., Kvien, I. (2006). "Manufacturing process of cellulose whiskers/polylactic acid nanocomposites," *Compos. Sci. Technol.* 66(15), 2776-2784.

Petersson, L., and Oksman, K., (2006) "Biopolymer based nanocomposites: comparing layered silicates and microcrystalline cellulose as nanoreinforcement," *Compos. Sci. Technol.* 66(13), 2187-2196.

Sain, M., and Bhatnagar, A. (2003). "Manufacturing of nanofibrils from natural fibres, agro based fibres and root fibres," *CA Patent Appl.* 2,437,616.

Sain, M., and Oksman, K. (2006). *Cellulose Nanocomposites-Processing, Characterization and Properties*, K. Oksman, and M. Sain, eds., American Chemical Society, Washington, DC.

Saint-Flour, C., and Papirer, E. (1982). "Gas-solid chromatography: a method of measuring surface free energy characteristics of short glass fibers through retention volumes measured near zero surface coverage," *Ind. Eng. Chem. Prod. Res. Dev.* 21, 666-669.

Schultz, J., Lavielle, L., and Martin, C. (1987). "The role of the interface in carbon fiber-epoxy composites," *J. Adhesion* 23, 45-60.

Thielmann, F. (2004). "Introduction into the characterization of porous materials by inverse gas chromatography," *J. Chromatogr. A.* 1037, 115-123.

Tshabalala, M. A. (1997). "Determination of the acid-base characteristics of lignocellulosic surfaces by inverse gas chromatography," *J. Appl. Polym. Sci.* 65, 1013-1020.

Wang, B., and Sain, M. (2007). "Dispersion of soybean stock-based nanofiber in a plastic matrix," *Polym. Int.* 56(4), 538-546.

Wang, B., Sain, M., and Oksman, K. (2007). "Study of structural morphology of hemp fiber from the micro to the nanoscale," *Appl. Compos. Mater.* DOI 10.1007/s10443-006-9032-9.

Wu, Y.-P., Jia, Q.-X., Yu, D.-S., and Zhang, L.-Q., (2004). "Modeling young's modulus of rubber-clay nanocomposites using composite theories," *Polym. Test.* 23: 903-909.